arXiv:cond-mat/0506337v1 [cond-mat.str-el] 14 Jun 2005

Efficient calculation of the antiferromagnetic phase diagram of the 3D Hubbard model

P. R. C. Kent,[1] M. Jarrell,[2] T. A. Maier,[3] and Th. Pruschke[4]

[1] *University of Tennessee, Knoxville, TN 37996*
[2] *Department of Physics, University of Cincinnati, Cincinnati, OH 45221*
[3] *Computer Science and Mathematics Division, Oak Ridge National Laboratory, Oak Ridge, TN 37831*
[4] *Institut für Theoretische Physik, Universität Göttingen, Friedrich-Hund-Platz 1, 37077 Göttingen, Germany*

(Dated: February 2, 2008)

The Dynamical Cluster Approximation with Betts clusters is used to calculate the antiferromagnetic phase diagram of the 3D Hubbard model at half filling. Betts clusters are a set of periodic clusters which best reflect the properties of the lattice in the thermodynamic limit and provide an optimal finite-size scaling as a function of cluster size. Using a systematic finite-size scaling as a function of cluster space-time dimensions, we calculate the antiferromagnetic phase diagram. Our results are qualitatively consistent with the results of Staudt et al. [Eur. Phys. J. B 17 411 (2000)], but require the use of much smaller clusters: 48 compared to 1000.

The accurate and efficient solution of lattice Hamiltonians such as the Hubbard model is a long standing challenge in the theoretical condensed matter community. These lattice models are routinely solved on a finite periodic lattice, for example with Monte Carlo, and the calculated properties extrapolated to the infinite limit. Due to the numerical expense in solving these models for large lattices, it is imperative to choose lattices that are efficient for the estimation and extrapolation of the physical properties of interest.

In this paper we use the Dynamical Cluster Approximation (DCA) [1, 2, 3] (for a review see [4]) to explore the antiferromagnetic instability in the 3D Hubbard model at half filling, with

$$H = -t \sum_{\langle ij \rangle, \sigma} c^{\dagger}_{i\sigma} c_{j\sigma} + U \sum_{i} (n_{i\uparrow} - \frac{1}{2})(n_{i\downarrow} - \frac{1}{2}) \,, \quad (1)$$

where $c^{(\dagger)}_{i\sigma}$ (creates) annihilates an electron with spin σ on site i, $n_{i\sigma}$ is the corresponding number operator, t the hopping amplitude between nearest neighbors $\langle i, j \rangle$ and U the on-site Coulomb repulsion. We solve this model on a series of finite clusters chosen according to the criteria proposed by Betts et al.[5, 6]. We obtain converged results extrapolating from clusters of up to only 48 sites, which are in agreement with the calculations of Staudt et al.[7], who used conventional cubic lattices of up to 1000 sites and obtained the Néel temperature via the specific heat.

To solve the Hamiltonian (1) we utilized the DCA [4]. For a $3D$ system the DCA maps the original lattice model onto a periodic cluster of size $N_c = L_c^3$ embedded in a self-consistent host. Thus, correlations up to a range $\xi \lesssim L_c$ are treated directly, while the longer length scale physics is described at the mean-field level. With increasing cluster size, the DCA systematically interpolates between the single-site dynamical mean-field result and the exact result, while remaining in the thermodynamic limit. We solve the cluster problem using Quantum Monte Carlo (QMC) [8]. At half-filling there is no QMC sign problem; the only systematic error in the Monte Carlo is the time step error, which can be extrapolated away.

In order to calculate the phase diagram of the system in the thermodynamic limit, we employ the scaling ansatz $\xi(T_{\rm N}^{\rm DCA}) = L_c$ where $T_{\rm N}^{\rm DCA}$ is the Néel temperature obtained from a DCA calculation with a cluster of linear cluster size L_c. This form is justified if we envision the lattice as perfectly tiled by a periodic array of non-overlapping clusters. This system becomes ordered when the antiferromagnetic correlations of the cluster reach the linear cluster size. According to this ansatz $\xi(T_{\rm N}^{\rm DCA}) \propto |T_{\rm N}^{\rm DCA} - T_{\rm N}|^{-\nu} \propto L_c$, so that

$$T_{\rm N}^{\rm DCA} = T_{\rm N} + B N_c^{-1/3\nu} \quad (2)$$

where $T_{\rm N}$ is the true antiferromagnetic transition temperature in the thermodynamic limit. The exponent is well-known for the 3D Heisenberg model, where one finds $\nu \approx 0.71$[9].

Betts et al. [5, 6] systematically studied the 2D and 3D Heisenberg models on finite size clusters and developed a grading scheme to determine which clusters should be used in finite size simulations. The main qualification is the "perfection" of the near-neighbor shells: a measure of the completeness of each neighbor shell compared to the infinite lattice. A perfect finite size cluster has all neighbor shells up to the k-th shell complete, the k-th shell is incomplete, and all shells k+1 and higher are empty. The absolute deviation from this criteria is defined as the imperfection. I.e. if the cluster neighbor configuration is as described, except that the k-1 shell is missing one entry, the cluster imperfection is one. The second qualification is the cubicity[6], $C = max(c_1, c_1^{-1}) max(c_2, c_2^{-1})$, where $c_1 = 3^{1/2} l/d$ and $c_2 = 2^{1/2} l/f$ are defined by the geometric mean of the lengths of the four body diagonals of the cluster, $d = (d_1 d_2 d_3 d_4)^{1/4}$, the six face diagonals $f = (f_1 f_2 f_3 f_4 f_5 f_6)^{1/6}$, and the edges $l = (l_1 l_2 l_3)^{1/3}$. $C = 1$ for a cube, so the deviation of C from one is a measure of the cubic imperfection. In finite size scaling calcu-

lations of the order parameter and ground state energy, they found that the results for the most perfect clusters fall on a scaling curve, while the imperfect clusters generally produce results off the curve. We generated additional 3D clusters following these guidelines for clusters larger than the 27 site clusters previously published[6], from which we adopt the labeling conventions and cluster geometries. In Table I we list clusters up to 70 sites, their perfection and cubicity. In each case, we chose either the bipartite (labeled B) or non-bipartite cluster (labeled A) with the smallest imperfection and cubicity closest to one, in this order of priority. For example, the 38 site cluster 38B is bipartite, perfect, consisting of only complete neighbor shells, and has a cubicity of 1.087. Since we are interested in a calculation of $T_{\rm N}^{\rm DCA}$, we utilized only bipartite clusters in the present calculations.

To obtain the antiferromagnetic phase diagram we performed a series of DCA calculations as a function of U/t, cluster size, and Monte-Carlo time step $\Delta\tau$. For a given U/t and cluster size, we calculated $T_{\rm N}^{\rm DCA}$ by finding the divergence of the staggered susceptibility as a function of $\Delta\tau$, and extrapolated the value obtained to $\Delta\tau = 0$. As an example, we show in Fig.1 the Néel temperature $T_{\rm N}^{\rm DCA}(\Delta\tau)$ for an 18 site cluster for $U/t = 8$. One finds a significant $\Delta\tau$ dependence which makes an extrapolation to $\Delta\tau = 0$ mandatory.

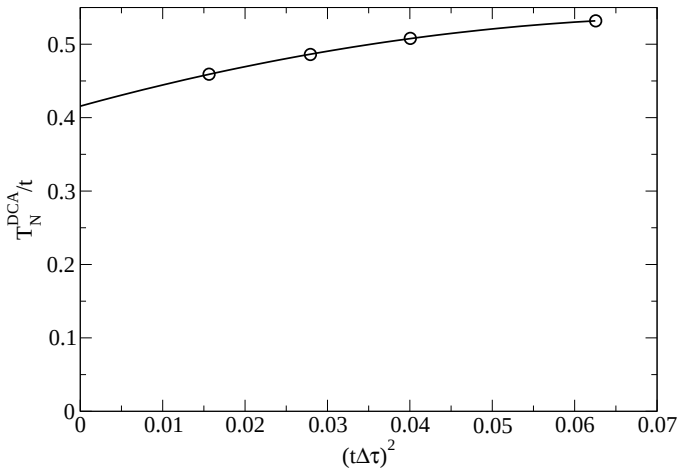

FIG. 1: T_N versus $\Delta\tau^2$ when $U/t = 8$ for cluster 18A

Performing this extrapolation for the series of bipartite clusters from Table I for $U/t = 8$, we obtain the values for $T_{\rm N}^{\rm DCA}$ collected in Fig. 2 (full circles). For comparison we also included the results for a finite $t \cdot \Delta\tau = 1/4$ (open circles). This unextrapolated data actually lies above the Heisenberg result of T/t=0.48. One clearly sees that a proper scaling to $\Delta\tau = 0$ is necessary to obtain both the correct qualitative *and* quantitative behavior of $T_{\rm N}^{\rm DCA}(N_c)$. The full curves in Fig. 2 were obtained with the scaling ansatz (2) using the ν for the 3D Heisenberg model. It yields a linear scaling curve within our error

N_c	$\vec{a}_1$	$\vec{a}_2$	$\vec{a}_3$	Imperfection	Cubicity
28A	(1, 1, 3)	(3,-1, 1)	(1, 2,-2)	0	1.063
28B	(1, 1, 2)	(3, 2,-1)	(1,-3, 2)	5	1.018
30A	(1, 2, 2)	(2, 2,-2)	(2,-2, 1)	0	1.007
30B	(1, 1, 2)	(3, 1,-2)	(3,-2, 1)	4	1.012
32A	(1, 1, 3)	(2, 2,-2)	(2,-2, 1)	0	1.022
32B	(1, 2, 3)	(2, 0,-2)	(2,-2, 2)	3	1.028
34A	(1, 1, 3)	(3,-2, 0)	(1, 2,-2)	0	1.009
34B	(1, 0, 3)	(2, 2,-2)	(1,-3,-2)	2	1.057
36A	(1, 2, 2)	(3, 0,-2)	(2,-2, 2)	0	1.004
36B	(1, 0, 3)	(3, 2,-1)	(2,-2,-2)	3	1.040
38A	(1, 1, 3)	(3, 1,-3)	(2,-2, 1)	0	1.002
38B	(1, 2, 3)	(3,-1,-2)	(2,-2, 2)	0	1.087
40A	(1, 2, 2)	(3, 1,-2)	(1,-3, 2)	0	1.003
40B	(1, 2, 3)	(2, 2,-2)	(2,-2, 2)	3	1.041
42A	(1, 2, 2)	(3, 0,-2)	(0, 3,-3)	0	1.005
42B	(1, 2, 3)	(3,-1, 2)	(2, 2,-2)	2	1.056
44A	(1, 2, 2)	(3, 2,-2)	(3,-2, 1)	0	1.010
44B	(1, 2, 3)	(3, 2,-1)	(2,-2, 2)	3	1.035
46A	(1, 1, 3)	(3, 2,-2)	(3,-2, 0)	0	1.014
46B	(1, 2, 3)	(3, 1,-2)	(2,-2, 2)	4	1.017
48A	(1, 1, 3)	(3, 2,-2)	(2,-3,-1)	0	1.009
48B	(1, 2, 3)	(3,-2, 1)	(2, 2,-2)	5	1.002
50A	(1, 1, 3)	(3, 2,-2)	(2,-3, 1)	1	1.005
50B	(1, 2, 3)	(3, 2,-1)	(2,-3, 1)	6	1.018
52A	(2, 2, 3)	(3, 2,-2)	(3,-2,-2)	1	1.109
52B	(1, 2, 3)	(3, 1,-2)	(2,-3, 1)	7	1.003
54A	(1, 2, 3)	(3, 0,-3)	(3,-2, 2)	2	1.063
54B	(1, 2, 3)	(3,-3, 0)	(2, 2,-2)	8	1.005
56A	(1, 1, 3)	(3, 2,-2)	(3,-3,-1)	3	1.003
56B	(1, 2, 3)	(3, 2,-3)	(3,-1, 2)	9	1.029
58A	(1, 1, 3)	(3, 2,-2)	(3,-3, 1)	3	1.014
58B	(1, 2, 3)	(3,-3, 2)	(2, 2,-2)	10	1.011
60A	(2, 0, 3)	(2, 3,-2)	(2,-3,-2)	4	1.001
60B	(1, 2, 3)	(3,-3, 2)	(2, 1,-3)	11	1.011
62A	(1, 3, 3)	(3, 2,-2)	(3,-3,-1)	5	1.087
62B	(1, 2, 3)	(3, 2,-1)	(3,-3, 2)	12	1.003
64A	(1, 2, 3)	(3, 1,-3)	(2,-3, 2)	6	1.013
64B	(1, 2, 3)	(3, 2,-3)	(2,-3, 1)	12	1.010
66A	(1, 3, 3)	(3, 3,-1)	(2,-3, 2)	5	1.067
66B	(1, 2, 3)	(3, 0,-3)	(3,-3, 2)	11	1.026
68A	(1, 3, 3)	(3, 3,-1)	(3,-2, 2)	4	1.055
68B	(1, 2, 3)	(3, 3,-2)	(2,-3, 3)	10	1.054
70A	(1, 3, 3)	(3, 3,-2)	(-2, 2,-3)	3	1.063
70B	(1, 2, 3)	(3, 3,-2)	(3,-2, 3)	9	1.034

TABLE I: 3D cluster geometries, imperfection and cubicity of the best non-bipartite (A clusters) and bipartite (B clusters). The a_i denote the cluster lattice vectors.

bars.

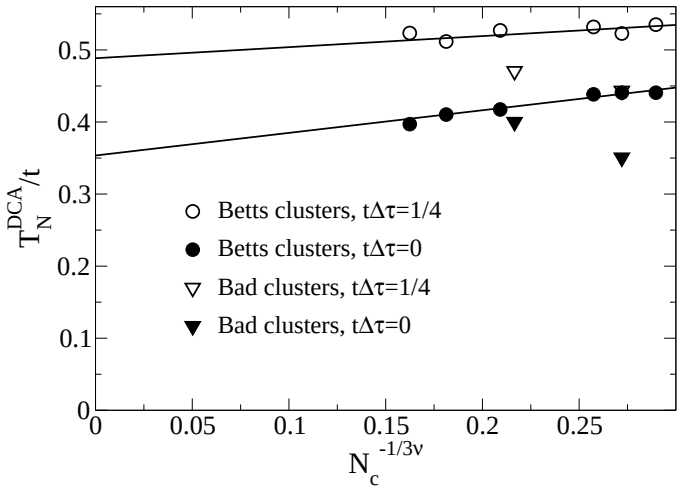

FIG. 2: Cluster size scaling of T_N when $U/t = 8$ and $t\Delta\tau = 1/4$ (open circles) and the result extrapolated to $t\Delta\tau = 0$ (full circles) as in Fig. 1.

To assess the value of Betts clusters, we also study two bad clusters, 16Z and 26Z, identified in Table II. Although these clusters are bipartite, they are highly imperfect. Both are missing independent neighbors in the first shell (each have 4; whereas a complete first shell has 6 neighbors). As a result of the periodic boundary conditions on the cluster, this causes the near-neighbor fluctuations to be over estimated. As a result, the estimates of T_N from these clusters, shown Fig. 2 for a finite $t \cdot \Delta\tau = 1/4$ (open triangles) and for the data extrapolated to $\Delta\tau = 0$ (filled triangles), fall well below the scaling curve established by the best cluster geometries listed in table I. In general, in this and in other calculations, we find that the less perfect clusters tend to overestimate the effects of fluctuations.

N_c	$\vec{a}_1$	$\vec{a}_2$	$\vec{a}_3$	Imperfection	Cubicity
16Z	(2, 0, 0)	(0, 2, 0)	(0, 0, 4)	7	1.209
26Z	(1, 2, 3)	(3, 3,-2)	(3,-2, 3)	14	1.295

TABLE II: 3D cluster geometries, imperfection and cubicity of two poor quality bipartite clusters.

Finally, Fig.3 displays the calculated antiferromagnetic phase diagram obtained from the DCA and extrapolated to $\Delta\tau = 0$ and $N_c = \infty$ (open circles with error bars). For comparison, we included results from other methods: The dynamical mean-field approximation (DMFA, full circles), Staudt et al.[7] (full curve), second order perturbation theory (SOPT, dotted curve)[10, 11], the Heisenberg model (dashed curve)[12] and the Weiss mean-field theory for the Heisenberg model (dash-dotted curve). We took $J = 4t^2/U$ for both Heisenberg calculations. The results from Staudt et al. are reproduced with good accuracy, but with much smaller clusters. The DMFA result is obtained through the methods described above when $N_c = 1$. Both the DMFA and the Weiss mean field are local approximations which neglect the effect of non-local fluctuations. As expected, they agree in the strong coupling regime, $U > 12t = W$ (W is the bandwidth). Both DMFA and SOPT are only accurate at small U/t, indicating that non-local fluctuations are not important for small U. At large U/t the DCA results for T_N approach the curve for the Heisenberg model, as expected. However, for intermediate and large values of U/W, the deviation between the present results and the mean-field results is as large as 30% or more, indicating that the effects of non-local fluctuations are significant.

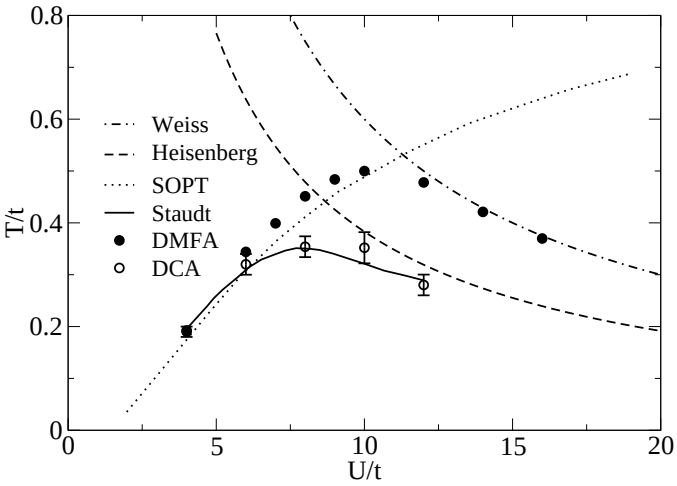

FIG. 3: Antiferromagnetic phase diagram of the 3D Hubbard model from our results and different approximations.

In conclusion, we have calculated the antiferromagnetic phase diagram of the 3D Hubbard model at half filling using the Dynamic Cluster Approximation and Betts clusters. Well converged results are found for relatively small cluster sizes due to the well-chosen geometries of these clusters. The dramatically increased efficiency of these clusters compared to typically used cluster geometries, such as cubic lattices, suggests that these clusters should be more widely used for lattice calculations.

We acknowledge useful discussions with J.P. Hague and G. Stewart. This research used computational resources of the Center for Computational Sciences, and was sponsored by the offices of Basic Energy Sciences and Advanced Scientific Computing Research, U.S. Department of Energy. Oak Ridge National Laboratory is managed by UT-Battelle, LLC under Contract No. DE-AC0500OR22725. This research was supported by the NSF Grant No. DMR-0312680 and supported in part by NSF cooperative agreement SCI-9619020 through resources provided by the San Diego Supercomputer Center.

[1] M. H. Hettler, A. N. Tahvildar-Zadeh, M. Jarrell, T. Pruschke, and H. R. Krishnamurthy, Phys. Rev. B **58**, R7475 (1998).

[2] M. H. Hettler, M. Mukherjee, M. Jarrell, and H. R. Krishnamurthy, Phys. Rev. B **61**, 12739 (2000).

[3] T. Maier, M. Jarrell, T. Pruschke, and J. Keller, Eur. Phys. J B **13**, 613 (2000).

[4] T. Maier, M. Jarrell, T. Pruschke, and M. Hettler, preprint cond-mat/0404055 (2004).

[5] D. D. Betts, H. Q. Lin, and J. S. Flynn, Can. J. Phys. **77**, 353 (1999).

[6] D. D. Betts and G. E. Stewart, Can. J. Phys. **75**, 47 (1997).

[7] R. Staudt, M. Dzierzawa, and A. Muramatsu, Eur. Phys. J. B **17**, 411 (2000).

[8] M. Jarrell, T. Maier, C. Huscroft, and S. Moukouri, Phys. Rev. B **64**, 195130 (2001).

[9] A. W. Sandvik, Phys. Rev. Lett. **80**, 5196 (1998).

[10] A. N. Tahvildar-Zadeh, J. K. Freericks, and M. Jarrell, Phys. Rev. B **55**, 942 (1997).

[11] P. G. J. van Dongen, Phys. Rev. Lett. **67**, 757 (1991).

[12] G. Rushbrooke, G. Baker, and P. Wood, in *PhaseTransitions and Critical Phenomena*, edited by C. Domb and M. Green (Academic Press, New York, 1974), vol. 3.